SCIENCE CHINA
Information Sciences

• RESEARCH PAPER •

April 2025, Vol. 68, Iss. 4, 142202:1–142202:13
https://doi.org/10.1007/s11432-024-4295-8

# Manipulate holistic cooperation of population game: optimal induction strategy for a few irrational agents in social networks

Zhen WANG, Peixuan SONG, Da-Tian PENG & Dengxiu YU*

*School of Cybersecurity, Northwestern Polytechnical University, Xi'an 710072, China*

Received 3 March 2024/Revised 15 May 2024/Accepted 10 July 2024/Published online 13 March 2025

**Abstract** In social networks, cooperation dilemmas among agents persist as a significant challenge. Existing research often emphasizes mild interactions among rational agents for autonomous cooperation, but it tends to overlook the impact of irrational agents' decisions, particularly under intentional inductions. This paper proposes an optimal induction strategy to enhance overall cooperation within the network, even when only one irrational agent is involved. We employ a continuous action iterative prisoner dilemma framework to model multi-agent games and utilize a tracker to minimize cooperation costs. A heuristic regulation algorithm is employed to generate optimal induction strategies, which may involve selecting a rational agent as a proxy for the irrational one. Through theoretical analysis using the Lyapunov direct method, we demonstrate the convergence of game dynamics despite the presence of irrational agents. Numerical results validate the effectiveness of our proposed strategy in promoting holistic cooperation. These findings highlight the vulnerability of social networks to external incentives and pave the way for further research into optimizing multi-agent cooperation dynamics.

**Keywords** population game, prisoner's dilemma, convergence, cooperation tightness, social network

**Citation** Wang Z, Song P X, Peng D-T, et al. Manipulate holistic cooperation of population game: optimal induction strategy for a few irrational agents in social networks. Sci China Inf Sci, 2025, 68(4): 142202, https://doi.org/10.1007/s11432-024-4295-8

## 1 Introduction

Recent studies have increasingly focused on the cooperative behaviors of rational agents within social networks and their broader implications [1–3]. A well-known illustration of these dynamics is the prisoner's dilemma, which effectively captures the tension between individual interests (betrayal) and societal welfare (cooperation) [4–6]. In this scenario, betrayal is the most advantageous option from each rational agent's perspective, regardless of other agents' decisions. Conversely, cooperation is deemed optimal from the whole social network's perspective. This disparity between local interests and global benefits leads to a widespread cooperation dilemma observed in real-world scenarios. Understanding this the cooperation dilemma is crucial for promoting holistic cooperative behavior within social networks and, by extension, society as a whole.

To solve the cooperation dilemma, two methods have been explored in existing research to sustain cooperation in social networks, even when cooperation costs are significant. The first approach focuses on delineating the mild interaction patterns among rational agents to foster intrinsic autonomous cooperation. For example, Ref. [7] proposed a game model incorporating reputation evaluation, which improves collective cooperation through reputation assessment. Ref. [8] clearly demonstrated how reputation and reciprocity influence the evolution of cooperation in social dilemmas. Moreover, as shown in [9], optimal control laws have been derived to promote cooperation by minimizing the overall cost function for each rational agent. In [10], a nonlinear dynamic model was used to depict the evolving interactions among multiple agents aiming to achieve cooperation. The second approach in this field focuses on crafting exogenous intentional induction strategies to manipulate population game cooperation. Although defection is often a rational choice for individuals, external incentives can significantly encourage cooperative behavior. For example, a novel class of zero-determinant strategies was proposed in [11,12], which influences

* Corresponding author (email: yudengxiu@nwpu.edu.cn)

 

decision-making in social networks by controlling the linear relationship between an agent's expected payoff and that of other players. In addition, cooperation commitment policies have been established for specific agents to offset cooperation costs in [13–15]. In [16], the asynchronous best-response dynamics in networks of anti-coordinating agents were studied, offering payoff incentives to achieve more stable system-wide outcomes. However, these previous studies in [9–16] only concentrate on rational agents, overlooking the potential for irrational agents to be attracted by external intentional inductions. Such agents might shift their decisions from betrayal to cooperation.

In addition, during exogenous induction operations, some rational agents may transition to irrational behavior, shifting from cooperation to betrayal. This transition can lead to induction failure and destabilize the cooperation state. In previous studies [17, 18], this issue has been addressed as node failure recovery. Ref. [17] verified the effectiveness of a dynamic model recovery strategy based on network state and topology. Ref. [18] introduced a local recovery model, where neighboring nodes engage in an invasive repair process starting from a seed node. Nevertheless, these node recovery strategies often fall short of swiftly restoring cooperative cohesion owing to the abrupt and widespread nature of betrayal by multiple irrational agents.

Building on previous investigations, this paper addresses their limitations by proposing an optimal induction strategy specifically targeting the influence of one or a few irrational agents. This strategy is crucial in understanding how holistic cooperation within a social network can be manipulated. As shown in [19–21], understanding the dynamics and evolution of population games is crucial for formulating effective induction strategies to enhance the holistic cooperation level in social networks. This paper explores the impact of irrational agents transitioning from cooperation to betrayal on the holistic cooperation within the network and offers an effective solution to the cooperation dilemma in population games. The main contributions of this paper are the following.

(i) Traditional prisoner's dilemma models typically represent binary decisions of cooperation or betrayal, inadequately describing the continuous decision-making processes in social networks consisting of multiple agents. To address this, we introduce the continuous action iterative prisoner dilemma (CAIPD) framework. This framework models the multi-agent population game, accurately characterizing the propagation of behaviors across the entire social network, where all agents are sensitive to external intentional inductions.

(ii) Large-scale population games often face the challenge of dimensionality explosion when computing an optimal induction strategy. We tackle this challenge by applying external optimal induction to a few, or even a single, irrational agent rather than all agents in the network. This allows these agents to manipulate holistic cooperation more effectively.

(iii) Previous node recovery strategies can barely address the abrupt betrayal of multiple irrational agents during optimal induction operations. To overcome this, we present a heuristic regulation algorithm that identifies a rational agent to act as a proxy for the irrational one, thereby restoring cooperative cohesion.

(iv) To justify the validity of our optimal induction strategy, we adopt the Lyapunov direct method to theoretically prove the dynamic convergence of the population game. Additionally, we conduct numerical simulations to illustrate the evolution of the population game toward tighter holistic cooperation.

The remaining structure of this paper is as follows: Section 2 introduces the CAIPD system model, providing a detailed description of the problem at hand. Section 3 discusses the development of optimal induction strategies, highlighting their potential to effectively guide the evolution of cooperative behaviors within the network. Section 4 designs a multi-agent control algorithm utilizing iterative control methods and examines the collective intelligence approach in scenarios where irrational agents choose betrayal. Section 5 introduces the results of simulation experiments, offering a thorough analysis of the outcomes. Section 6 concludes this work.

## 2 System model and problem formulation

### 2.1 CAIPD model

In the CAIPD model [22], a total of $N$ individuals are strategically located across $N$ vertices $v_i \in \mathcal{V}$ for $i = \{1, \ldots, N\}$ within a graph $\mathbb{G} = (\mathcal{V}, \mathcal{W})$. The symmetric $N \times N$ adjacency matrix $\mathcal{W} = [w_{ij}]$, where $w_{ij} \in \{0, 1\}$, characterizes the interactions among agents from $i$th to $j$th and encapsulates all

$w_{ii} = 0$. Unlike the traditional prisoner's dilemma model, which offers only binary choices, the CAIPD allows for a continuous spectrum of cooperative behaviors. Each agent's state $x_i$ ranges from $x_i$ =0 signifying complete defection, to $x_i = 1$ representing complete cooperation. In this scenario, a player incurs a cost $cx_i$, while the adversary receives a benefit $bx_i$, where $b > c$. Consequently, a defector (i.e., $x_i = 0$) bears no cost and imparts no benefits. Consequently, the agent's fitness $i$ is calculated as $f_i = -\deg[v_i]\, cx_i + b\sum_{j=1}^{N} w_{ij}x_j$, where $\deg[v_i]$ signifies the count of neighbors surrounding $v_i$. Within the CAIPD framework, rational agents engage in imitation dynamics, emulating the strategies of their neighbors in proportion to their fitness levels. Agent $i$ embraces the strategy of its $j$th neighbor with a degree of influence amounting to $p_{ij} = w_{ij} \cdot \text{sigmoid}(\beta(f_j - f_i))$, where $\beta$ determines the sensitivity of strategy adoption to advantageous strategies.

A network is characterized by a state $x$ and topology $\mathbb{G}$, defined as $\mathbb{G}_x = (\mathbb{G}, x)$, where $x = [x_1, x_2, \ldots, \mathrm{s}x_N]^\top$. This network $\mathbb{G}_x$ can be viewed as a dynamic system, where $x$ evolves in response to a nonlinear mapping $\dot{x} = [h_1(x), \ldots, h_N(x)]^\top$, where $h_i(x)$ represents the dynamics of the $i$th entity within $\mathbb{G}_x$. Specifically, $h_i(x) = \frac{1}{\deg[v_i]}[\sum_{j=1}^{N} p_{ij}(x_j(t) - x_i(t))]$. This dynamic system can be reformulated into a standard structure by introducing the Laplacian operator, $\mathcal{L}(\cdot)$, defined as follows:

$$\dot{x}(t) = -\mathcal{L}[x(t)]\, x(t), \tag{1}$$

where

$$\mathcal{L}_{ij} = \begin{cases} -p_{ij}/\deg[v_i], & \text{if } i \neq j, \\ \sum\limits_{j=1}^{N} p_{ij}/\deg[v_i], & \text{if } i = j. \end{cases} \tag{2}$$

Within the model of CAIPD, fitness updates occur at every time step $t$. In order to enhance the authenticity of influencing behavior and improve the optimal induction strategy, we introduce the concept of dwell time $\tau$, as originally proposed in [13,23], and seamlessly integrate it into the CAIPD model. This adaptation enables us to transform the model described in [22] into a piecewise time-invariant structure:

$$\dot{x}(t) = -\mathcal{L}_k x(t), \tag{3}$$

where $\mathcal{L}_k = \mathcal{L}(x(k\tau))$, signifying $k\tau < t < (k+1)\tau$, and $k = 1, 2, \ldots$ It is evident that when $\tau \to 0$, the formulation in (3) simplifies to the one presented in [14], where as for $\tau \to \infty$, the outcome resembles a static consensus model as elaborated in [24].

In a general context, a non-linear dynamic system is described by $\dot{x} = f(t; x, u)$, in which state variables $x$ undergo non-linear transformations $f_i$ over $i \in \{1, \ldots, N\}$. In the case of linear and time-invariant (LTI) systems, the framework simplifies to

$$\dot{x} = Ax + Bu, \tag{4}$$

where $x = [x_1, x_2, \ldots, x_N]^\top$ and $u = [u_1, u_2, \ldots, u_q]^\top$ symbolize state and input variables, respectively, with matrices $A$ and $B$ serving as transformation and manipulation matrices. In control design, the goal is to develop a feedback controller capable of driving the system toward a predefined cooperative state. While delving into the intricate mechanisms of these methodologies exceeds the scope of this manuscript, the focus remains on assessing stability and convergence within dynamical systems. Stability is examined in the proximity of equilibrium points (i.e., points where $\dot{x} = 0$). To quantitatively describe these neighborhoods, an unbounded region, defined as $\mathcal{B}(\bar{x}, \epsilon)$, centered around $\bar{x}$, and characterized by a radius of $\epsilon$, (i.e., the set $\left\{x \in \mathbb{R}^d : \| x - \bar{x} \| < \epsilon\right\}$, where $\| \cdot \|$ represents the $L_2$-norm) is defined. Lyapunov stability can then be expressed as follows.

**Definition 1** (Lyapunov stability)**.** An equilibrium point $x_e$ of a nonlinear system is considered Lyapunov stable if, for every $\epsilon > 0$, there exists $a\delta > 0$ such that $\bar{x} \in \mathcal{B}(x_e, \delta) \Rightarrow f(t; \bar{x}, 0) \in \mathcal{B}(x_e, \epsilon)$ for all $t \geqslant 0$.

Lyapunov's direct approach utilizes the temporal rate of change within a potential function to verify Lyapunov stability. Specifically, a Lyapunov function is introduced as $V(x) : \mathbb{R}^N \to \mathbb{R}$ where $V(x) \geqslant 0$ holds true with equivalence solely in cases where $x = 0$. A system is asymptotically stable in the context of Lyapunov when $\frac{\mathrm{d}}{\mathrm{d}t}V(x) \leqslant 0$ with equality solely established if and only if $x = 0$.

### 2.2 Problem formulation

In the realm of linear quadratic tracking, the goal is to regulate a dynamical system structured as (4) to trace a designated reference signal $\bar{y}$, as formulated by

$$\dot{z} = Fz, \bar{y} = Hz, \tag{5}$$

where $z$ represents the internal state vector, $\bar{y}$ signifies the system's output, and $z(t_0) = z_0$ stands as the initial state. To address this quandary, the subsequent augmented system is introduced, encompassing the dynamic traits of both the primary and tracker dynamics:

$$\dot{\tilde{x}} = \tilde{A}\tilde{x} + \tilde{B}u \tag{6}$$

with

$$\tilde{A} = \begin{bmatrix} A & 0 \\ 0 & F \end{bmatrix}, \quad \tilde{B} = \begin{bmatrix} B \\ 0 \end{bmatrix}, \tag{7}$$

and $\tilde{x} = [x, z]^\top$. In order to encompass the resulting tracking discrepancy, the subsequent cost function is formulated:

$$\mathcal{J} = \int_{t_0}^{\top} \left[\tilde{x}^\top \tilde{Q}\tilde{x} + u^\top Ru\right] \mathrm{d}t \tag{8}$$

with

$$\tilde{Q} = \begin{bmatrix} Q & -QH \\ -H^\top Q & H^\top QH \end{bmatrix}, \tag{9}$$

where $A$ is the augmented state cost matrix, and $Q$ and $R$ represent the state and input cost matrices, respectively. The primary objective lies in determining $u = u^\star$ that minimizes the cost function delineated in (5). The optimal induction strategy can be achieved using $u^\star(t) = K_1(t)\, x(t) + K_2(t)\, z(t)$:

$$J(u) = \int_0^\infty \left(x^\top Qx + u^\top Ru + 2x^\top Nu\right) \mathrm{d}t \tag{10}$$

under the constraint of the system dynamics in (4). Alongside the state-feedback gain $K$, the linear quadratic regulator (LQR) also provides the outcome $S$ derived from the correlated Riccati equation:

$$A^\top S + SA - (SB + N) R^{-1} \left(B^\top S + N^\top\right) + Q = 0, \tag{11}$$

and the eigenvalues of the closed-loop system $e = \mathrm{eig}(A - B \cdot K) \cdot K$ are computed from $S$ through

$$K = R^{-1} \left(B^\top S + N^\top\right). \tag{12}$$

In the case of a discrete-time state-space model, $u[n] = -Kx[n]$ minimizes

$$J = \sum_{n=0}^{\infty} \left\{x^\top Qx + u^\top Ru + 2x^\top Nu\right\} \tag{13}$$

subject to $x[n+1] = Ax[n] + Bu[n]$.

$[K, S, e] = \mathrm{LQR}(A, B, Q, R, N)$ serves as a corresponding notation in continuous-time models characterized by dynamics $\dot{x} = Ax + Bu$.

The matrix $N$ is omitted here; i.e., $N$ is set to 0.

**Definition 2** (Agent type)**.** The agents are classified into two types: rational agents, who respond to external influences and make decisions based on logical reasoning and analysis, and irrational agents, who resist external influences, disregard the broader context, and tend to make decisions that lead to betrayal.

**Control objective.** To guide the information diffusion process, we employ optimal control theory. Specifically, we design a linear quadratic regulator to influence the decisions of a few irrational agents. These decisions are then propagated through the learning mechanisms of neighboring agents within the CAIPD model. This approach, which progresses from individual to collective influence, enables us to rapidly influence each agent in the network, thereby encouraging the entire network to adopt predesigned cooperative behaviors.

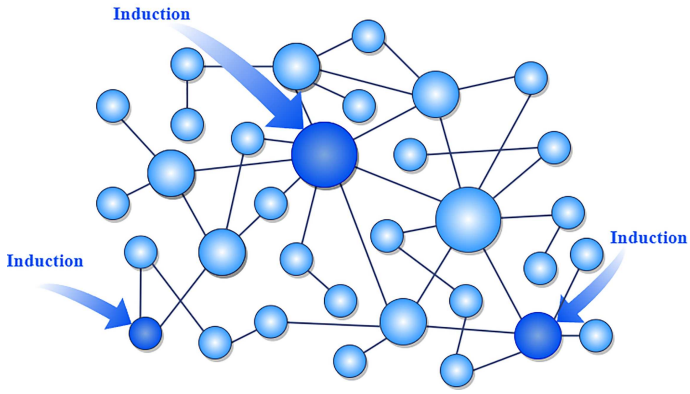


**Figure 1** Network affected by external influences. Light blue nodes represent normal agents, dark blue arrows represent induction, and dark blue nodes represent influenced rational agents.

## 3 Optimal induction strategy

Using the LQR controller discussed previously, we can strategically influence a select group of irrational agents within a social network, thereby guiding their decision-making processes. This involves introducing control signals $L \leqslant N$, expressed as $u_1, u_2, \ldots, u_L$, to influence supervised agents $x_1, x_2, \ldots, x_L$, thus affecting the development of the network following the CAIPD model. These signals may originate from external sources such as media outputs, government policies, or even influential leaders outside the network. In a formal manner, considering the CAIPD model $\dot{x} = -\mathcal{L}_k x$ as specified in (3), the integral of external influence can be expressed as follows:

$$\dot{x} = -\mathcal{L}_k x + Bu, \tag{14}$$

where $u = [u_1, u_2, \ldots, u_L]$ represents a control signal vector, and

$$B = \begin{bmatrix} I_{L\times L} \\ 0_{(N-L)\times L} \end{bmatrix} \tag{15}$$

represents the input matrix. Figure 1 depicts a visual representation of the network affected by external factors, with influenced rational agents highlighted in blue.

The primary objective of this study is to achieve a consensus across the network, expressed as $x_f = x^\star 1$, where $x^\star$ symbolizes the targeted level of cooperation. The condition under which $x_f$ is attainable at a specific time $t_0$ is formally defined as follows.

**Definition 3** (Reachability)**.** A state $x_f$ is considered attainable at time $t_0$, if there exists a control input $u_r(t)$ such that $x_f = \lim_{t\to\infty} x(t; t_0, x_0, u_r(t))$, where $x_0 = x(t_0)$.

Building on these definitions, the subsequent theorem is presented to demonstrate the reachability of any attainable consensus (i.e., $0 \leqslant x^\star \leqslant 1$) when a single individual is controlled.

**Theorem 1** (Reachability of agreements)**.** In the context of the CAIPD model, as stated in (14), enhancing external influence enables the attainment of any feasible consensus $0 \leqslant x^\star \leqslant 1$ at time $t_0$ for any initial state $x_0$. This is achieved by exerting control over a single manipulated individual $x_c$ through an appropriate control input:

$$u_r = \begin{cases} -\epsilon \cdot \operatorname{sgn}(e) + B^\top \mathcal{L}_k x, & \text{if } e \neq 0, \\ B^\top \mathcal{L}_k x, & \text{if } e = 0 \end{cases} \tag{16}$$

with $\epsilon > 0$ and error defined as $e = x_c - x^\star$. Then

$$\lim_{t\to\infty} x(t; t_0, x_0, u_r(t)) = x^\star 1. \tag{17}$$

*Proof.* We have decomposed the control process into two distinct stages. The first stage involves driving the network toward a manifold, enabling the influenced rational agent to reach a consensus value (i.e.,

$x_c \to x^\star$). In the second phase, the goal is to maintain the system on that manifold (i.e., $e = 0$) by ensuring $\dot{e} = 0$. Let us consider the potential Lyapunov function $V = 0.5e^2$. It is evident that $V \geqslant 0$, with equality only occurring when the influenced rational agent achieves consensus (i.e., $e = 0$), in which case $V = 0$. The time derivative of this candidate function is

$$\dot{V} = e\dot{e} = e\dot{x}_c = e\left(-B^\top \mathcal{L}_k x + u\right). \tag{18}$$

Substituting the control input $u_r$ from (13) for $e \neq 0$ into the aforementioned equation yields

$$\dot{V} = e\left(-\epsilon \cdot \operatorname{sgn}(e)\right) = -\epsilon\,|e|\,, \tag{19}$$

where $|\cdot|$ represents the magnitude of a scalar. Consequently, following Lyapunov's direct approach, if $\epsilon > 0$, then $V$ will eventually reach a value of zero in a finite time span, thereby yielding $e = 0$. This marks the culmination of the initial stage within the control procedure.

During the subsequent stage, it is imperative to maintain the network within the $e = 0$ manifold. The rate of change of the error signal is calculated as

$$\dot{e} = \dot{x}_c = -B^\top \mathcal{L}_k x + u. \tag{20}$$

By substituting the control input $ur$ from (16) into (20) and setting $e = 0$, we derive $\dot{e} = \dot{x}c = 0$. This ensures that the system strictly adheres to the $e = 0$ manifold, effectively maintaining equilibrium. To simplify our analysis without any loss of generality, we assume that the manipulated individual corresponds to the initial agent within the CAIPD model.

With this assumption, the network can be elegantly represented in the following format:

$$\frac{\mathrm{d}}{\mathrm{d}t}\begin{bmatrix} x_c \\ x_2 \\ x_3 \\ \vdots \\ x_N \end{bmatrix} = \begin{bmatrix} 0 & 0 & \dots & 0 \\ \mathcal{L}_{k_{21}} & \mathcal{L}_{k_{22}} & \dots & \mathcal{L}_{k_{2N}} \\ \mathcal{L}_{k_{31}} & \mathcal{L}_{k_{32}} & \dots & \mathcal{L}_{k_{3N}} \\ \vdots & \vdots & \ddots & \vdots \\ \mathcal{L}_{k_{N1}} & \mathcal{L}_{k_{N2}} & \dots & \mathcal{L}_{k_{NN}} \end{bmatrix} \begin{bmatrix} x^\star \\ x_2 \\ x_3 \\ \vdots \\ x_N \end{bmatrix}. \tag{21}$$

The CAIPD model properties lead to a novel state space matrix that is diagonally dominant and characterized by non-positive diagonal components. Furthermore, in the corresponding network graph, the manipulated agent is the sole node without inbound connections. Consequently, during the subsequent control phase, a network forms a spanning tree with the manipulated agent as the root. Based on established findings [10], the network ultimately attains a consensus. This means that $\lim_{t\to\infty} x_i(t) = \lim_{t\to\infty} x_c(t) = x^\star$, thereby concluding the proof.

While any predesigned cooperation can be achieved using external influences as defined in (21), there are two challenges yet to be addressed. First, the described approach relies on controlling a single manipulated irrational agent, which limits its applicability to more complex multi-agent control scenarios. Second, there is no systematic procedure for determining the optimal value of $\epsilon$, a parameter that significantly influences the effectiveness of control and convergence speed. To address these challenges, solutions based on optimal induction strategies are proposed.

## 4 Node control and failure recovery algorithm

### 4.1 Multi-node control algorithm

This section expands on the previously discussed methods to cover scenarios involving multiple agents in a social network influenced by external factors. Specifically, we broaden the scope to cover situations where direct real-time measurements of state values or the actual system's dwell time, $\tau$, are not readily available. This expansion leads to the development of an optimal induction strategy $u^\star$, which is grounded in the initial system configuration and an evaluation dwell time $\tau_{\text{eval}}$, serving as an approximation of the true dwell time $\tau_{\text{eval}}$.

This meticulously designed induction strategy aims to guide the system toward achieving an arbitrary consensus $x^\star$ within a finite time frame $T$. The dynamics governing the estimated state vector $\hat{x}$ can be mathematically represented as follows:

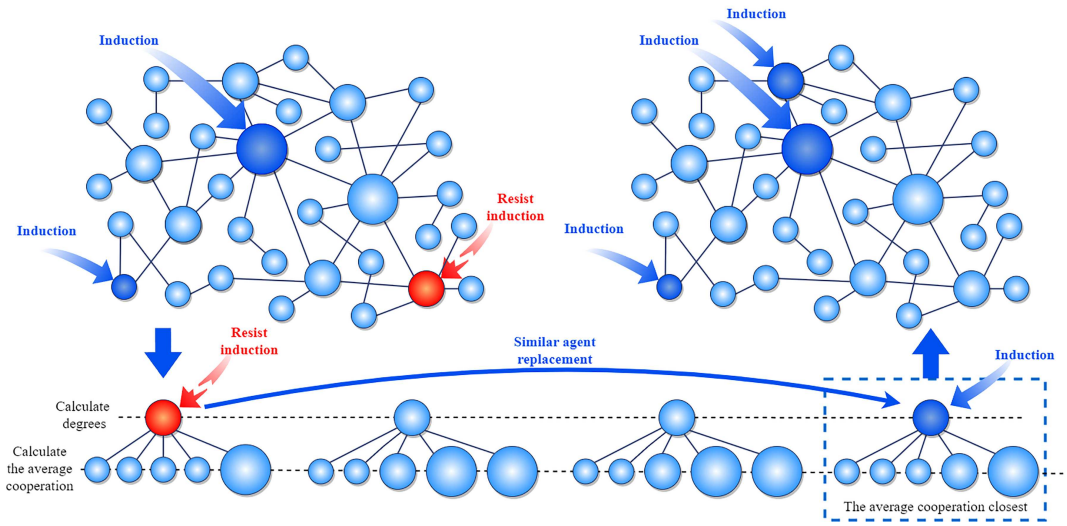


**Figure 2** Red nodes represent irrational agents that have betrayed. Red arrows represent resisting induction. After system failure recovery, a new social network will be generated.

$$\begin{cases} \dot{\hat{x}}\left(t\right) = -\hat{\mathcal{L}}_j \hat{x}\left(t\right) + B u_j\left(t\right), \\ \hat{x}\left(t_0\right) = x\left(t_0\right), \end{cases} \tag{22}$$

for $t_{j-1} < t \leqslant t_j$, where $j = 1, 2, \ldots, \frac{T}{\tau_{\text{eval}}}$ and $t_j = j \cdot \tau_{\text{eval}}$.

$\hat{\mathcal{L}}_j$ is a constant Laplacian matrix derived based on $\hat{x}\left(t_{j-1}\right)$. The cost function employed to compute the optimal induction strategy within the $j$th time segment is described as follows:

$$\mathcal{J}_j = \int_{t_j}^{\top} \left[\tilde{x}^{\top} \tilde{Q} \tilde{x} + u_j^{\top} R u_j\right] \mathrm{d}t, \tag{23}$$

where $\tilde{Q}$ and $R$ retain the same definitions as in (8), with $H = I_{N\times N}$, and $\tilde{x} = \left[\hat{x}, x^{\star}1\right]^{\mathrm{T}}$ stands for the augmented state vector. The objective is to determine $u_j^{\star}\left(t\right)$ in a manner that minimizes the cost function outlined in (23) for each $j$. According to (23), the optimal control law becomes

$$u_j^{\star}\left(t\right) = K_{j_1}\left(t\right)\hat{x}\left(t\right) + K_{j_2}\left(t\right)x^{\star}1. \tag{24}$$

Given the provided initial states, network topology, and predetermined parameters, the controller furnishes control dynamics $K_{j_1}\left(t\right)$ and $K_{j_2}\left(t\right)$ for $j = 1, 2, \ldots, \frac{T}{\tau_{\text{eval}}}$, subsequently employed in the derivation of the control input as follows:

$$u^{\star}\left(t\right) = K_{j_1}\left(t\right)x\left(t\right) + K_{j_2}\left(t\right)x^{\star}1, \tag{25}$$

for managing the actual network equation (24) during $t_{j-1} < t < t_j$ for each $j$.

### 4.2 Failure recovery algorithm

Furthermore, in scenarios similar to those depicted in Figure 2, we consider the irrational agents in the network that are influenced by external factors. To address this issue, we introduce the concept of agent degree difference, denoted by $\delta$. When identifying uncontrolled agents, we perform a comparative analysis to examine the relationship between the degrees of these agents and those of the remaining regular agents. If the degree difference is below a predefined $\delta$ threshold, we consider these agents as potential candidates for similarity. Subsequently, we calculate the average cooperativeness of all agents connected to the uncontrolled agents and compare it with the average cooperativeness of all agents connected to the potential similar candidates. The potential similar agent demonstrating the highest degree of similarity is then selected as the replacement agent. The detailed implementation process can be found in Algorithm 1.

The objective is to develop a systematic and adaptable method to address failures caused by the betrayal of irrational agents in the network. This approach not only identifies potential replacement

**Algorithm 1** Failure recovery algorithm after irrational agents out of control.

**for** $i$=1 to $n$ **do**
  For each irrational agent $i$, calculate the average cooperation degree of its connected agents;
  **for** $j$=1 to $n$ **do**
    Filter out agents $j$ with similar degrees to agent $i$ by calculating $\delta$, ($\delta$ refers to the degree difference between agent $i$ and agent $j$);
    **if** $\delta < 3$ **then**
      Select this potential similar agent $j$. Calculate the average cooperation degree of the connecting agents of the potential similar agent $j$;
    **end if**
    Compare the average cooperation degree of the connection agents with agent $i$, and select agent $j$ with the smallest difference as the replacement agent;
  **end for**
  Count the replacement agents $j$ of all irrational agents $i$ and replace them.
**end for**

agents but also ensures that the selected replacement agents closely match the original uncontrolled agents in terms of characteristics and cooperation patterns. This enhances the robustness and effectiveness of inductive strategies in dynamic environments.

If agent $i$ is affected by external factors and becomes unreliable, the selection process for potential similar agents is as follows:

$$|\deg(v_i) - \deg(v_j)| < \delta, i \neq j. \tag{26}$$

All potential similar agents $j$ that meet the agent degree criteria can be selected. The next step involves calculating the average collaboration degree of the connected agents:

$$x_i{}^* = \frac{\sum_{j=1}^{N} w_{ij} x_j}{\deg(v_i)}. \tag{27}$$

The agent $j$ with the smallest difference in average collaboration $|x_i{}^* - x_j{}^*|$ is selected as the similar replacement agent.

## 5 Simulation results

In this section, we present numerical experiments to validate our proposed CAIPD model, the induction strategy for promoting predesigned cooperation in social networks, and the mechanism for replacing betrayal agents.

### 5.1 Experiment settings

The performance of the provided incremental controller has been rigorously evaluated through a series of numerical simulations based on a network model. Specifically, we employed the Barabsi-Albert scale-free model [25] as the foundation for our experiments, renowned for its ability to capture the characteristics of real-world systems. In this section, we established a social network model comprising 50 internal agents and conducted a comprehensive validation of the numerical results from four different perspectives.

To ensure the smooth generation of control signals in the cost functions of (8) and (23) for the optimal controller, we have set the values of $Q$ and $R$ as follows: $Q = I \times 0.08$ and $R = I \times 1$.

### 5.2 Numerical experiments and analysis

#### 5.2.1 *Number of control nodes comparison*

This section first compares the changes in overall cooperation in the network when influence is applied to a single agent versus multiple agents. The analysis reveals how different influence strategies affect cooperation dynamics within the network.

In this comparative study, the final goal is achieving complete cooperation among all individuals $x^\star = 1$. Comparing Figures 3(a) and (b), a noteworthy observation emerges: when a single agent is affected, the cooperation level of the entire network converges slowly, reaching full cooperation at time 700. Conversely, when multiple agents are affected, the network quickly converges to the predesigned cooperative state, achieving full cooperation by time 250. This finding clearly demonstrates that exerting external influences on multiple agents significantly accelerates the convergence of network collaboration.

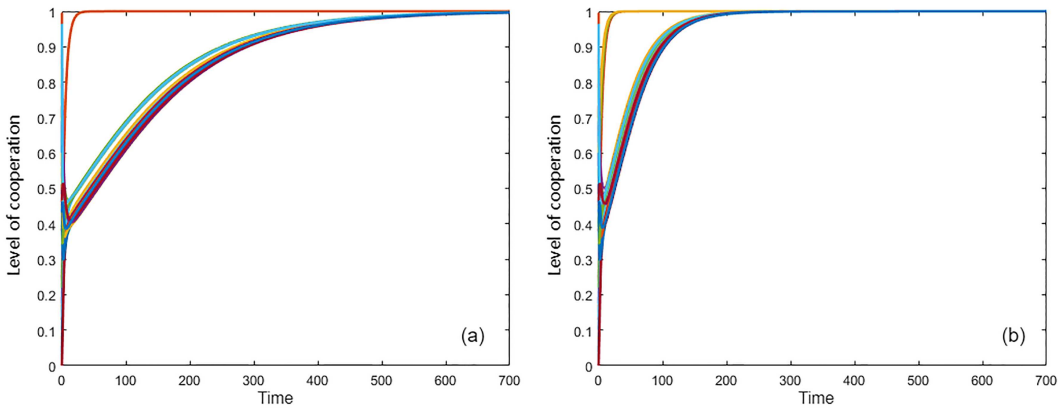


**Figure 3** (Color online) Overall cooperative status of the network when affecting different numbers of agents. (a) Single agent; (b) multiple agents.

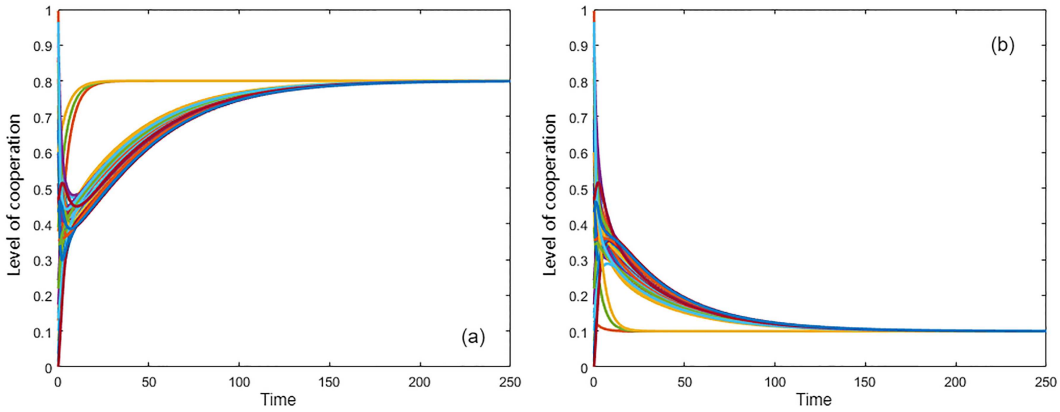


**Figure 4** (Color online) Cooperation status of the network changes. (a) The predesigned cooperation is $x^\star = 0.8$; (b) the predesigned cooperation is $x^\star = 0.1$.

### 5.2.2 *Predesigned cooperation comparison*

This part investigates the network's cooperation status under different predesigned cooperation scenarios. This exploration facilitates the evaluation of the controller's adaptability across different cooperation scenarios and its ability to achieve predefined cooperation levels.

In this comparative analysis, the predesigned cooperation settings require that all individuals fully cooperate $x^\star = 1$, and all agents partially cooperate $x^\star = 0.8$, $x^\star = 0.1$. By comparing Figures 3(b), 4(a), and 4(b), an important conclusion is drawn: the network can achieve any predesigned level of cooperation.

### 5.2.3 *Energy consumption comparison*

In this comparison, we plan to use optimal and traditional controllers to induce cooperation in social networks. By comparing the energy consumption of different controllers under identical conditions, we demonstrate the advantages of the optimal controller.

We designed a backstepping controller as a benchmark, with the control function as follows:

$$u\left(t\right) = \frac{-\widehat{\mathcal{L}}x\left(t\right) - kx\left(t\right)}{B}, \tag{28}$$

where $u(t)$ is the input of the backstepping controller, while $\widehat{\mathcal{L}}$ is represented in (2).

By comparing Figures 4(a) and 5, we observe that at time 250, both the optimal and backstepping controllers successfully induce the network to achieve the predesigned cooperation level of $x^\star = 0.8$.

To highlight the differences between these controllers, we compared the energy consumption while achieving the same control effects. Specifically, we recorded the absolute value of the input from each

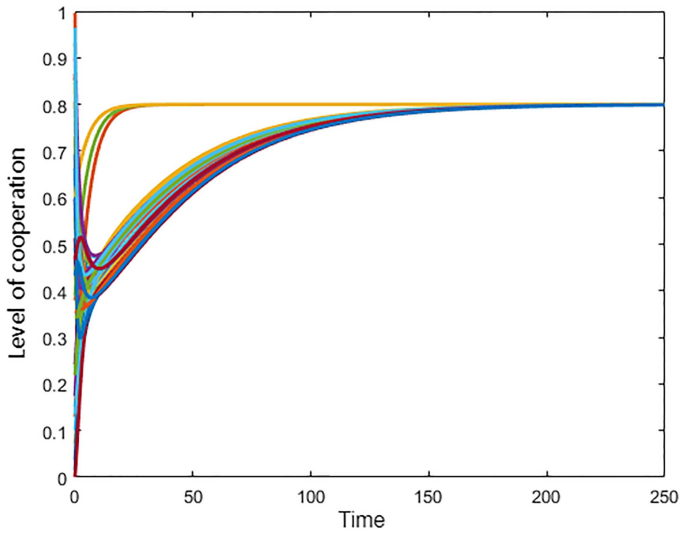


**Figure 5** (Color online) Use a backstepping controller to induce the network to reach the predesigned cooperation $x^\star = 0.8$.

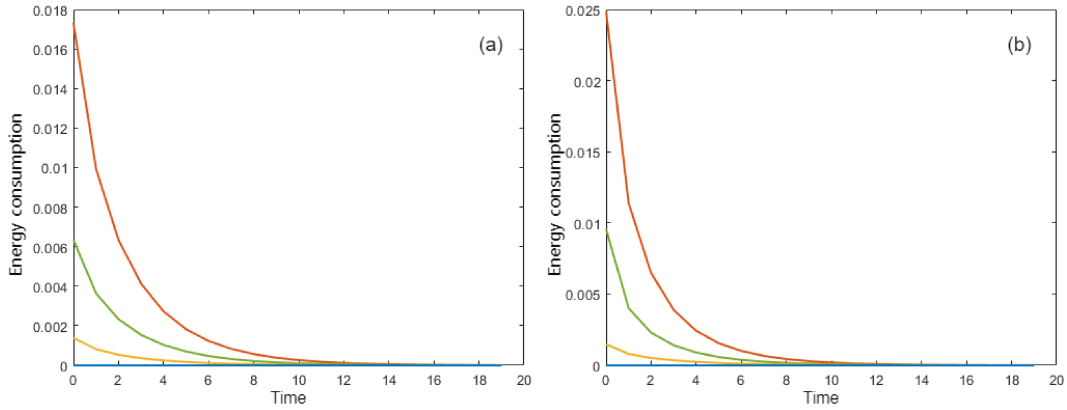


**Figure 6** (Color online) Square of the energy consumption required when using different controllers to induce the network to reach the predesigned cooperation $x^\star = 0.8$. (a) The optimal controller; (b) the backstepping controller.

controller to each agent influenced by external factors during each iteration. This data was used to construct Figure 6, which illustrates energy consumption over time.

Although both the optimal and backstepping controllers can effectively induce network cooperation, ensuring efficient information transmission and collaborative work, their energy consumption differs greatly. Comparing Figures 6(a) and (b), we observe that for the same control effects, the energy required by the optimal controller is approximately 0.75 of that required by the backstepping controller. This observation highlights the superiority of the optimal controller as it can significantly reduce energy consumption while maintaining performance. Consequently, the optimal controller offers greater cost-effectiveness and sustainability, making it the preferred choice in practical applications.

### 5.2.4 *Failure recovery comparison*

In this section, we facilitate the observation of changes before and after the replacement of uncontrolled agents by setting the values of $Q$ and $R$ as follows: $Q = I \times 0.01$ and $R = I \times 1$. The parameter transformation of $Q$ and $R$ is meant to enhance experimental demonstration without affecting the comparative results.

Initially, we examine scenarios involving irrational agents before the controller starts running. We designed two groups for this purpose: one where affected rational agents operate without fault and another where irrational agents undergo a betrayal and subsequent fault recovery. The first group serves as a control group, allowing us to better understand the suitability of the controller's failure recovery mechanism.

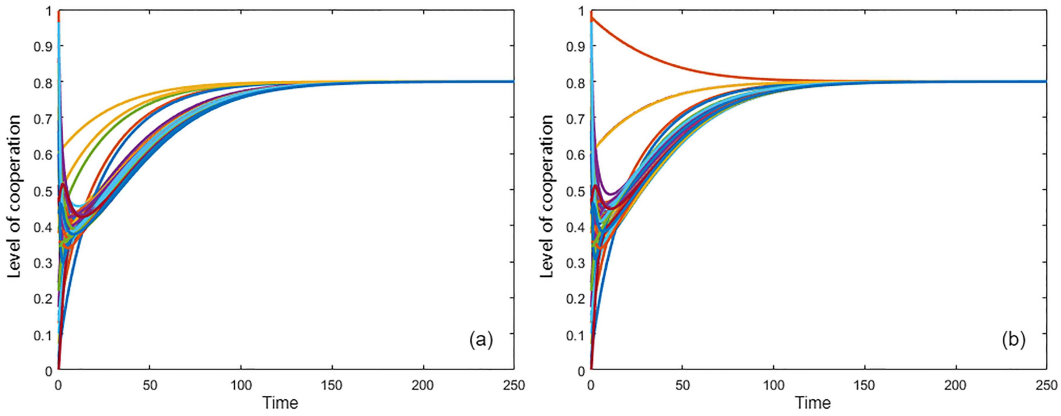


**Figure 7** (Color online) When the predesigned cooperation is $x^\star = 0.8$, the cooperation status of the network changes. (a) Five agents are affected; (b) two irrational agents are replaced.

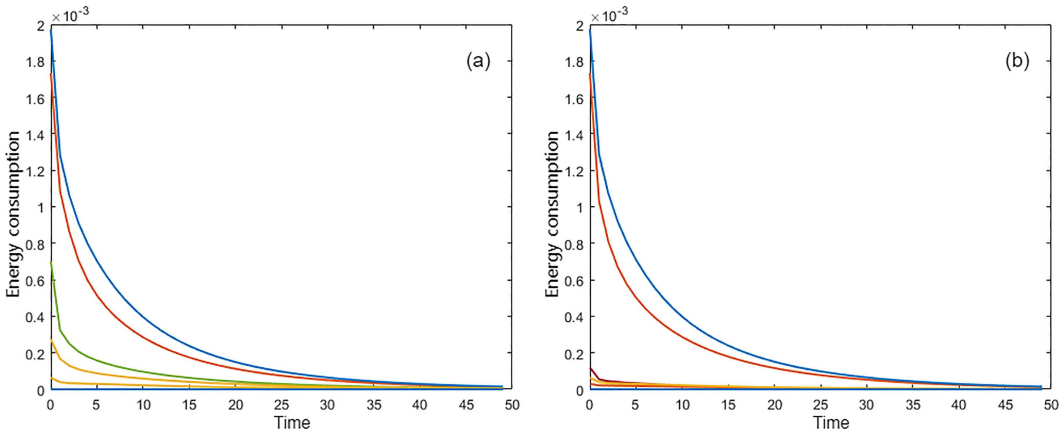


**Figure 8** (Color online) Square of the energy consumption required. (a) Five agents are affected; (b) two irrational agents are replaced.

In this comparison, we simulated a social network scenario featuring 5 external influence agents, as shown in Figure 7(a). In this scenario, two irrational agents are betrayed and then replaced by rational agents with similar characteristics, as shown in Figure 7(b). By comparing Figures 7(a) and (b), we can draw the following conclusion: before and after the replacement of these influenced, the social network successfully achieves the predesigned cooperation level. Importantly, the convergence time for cooperation remains consistent in both cases.

In addition, by comparing Figures 8(a) and (b), we observe that the energy consumption of the entire network remains largely unchanged before and after the fault recovery mechanism is activated. We also explore the performance of the controller before and after agent betrayal recovery during operation.

In this comparison, we simulated a social network scenario featuring 5 external influence agents. At time 30, two irrational agents betray, and then we observe the effects after these agents are replaced by rational counterparts with similar characteristics, as shown in Figure 9. By observing the changes in the network cooperation status before and after time 30 from Figure 9, we can draw the following conclusion: During controller operation, before or after the betrayal and replacement of the affected agents, the network consistently achieves the predesigned cooperation level.

By monitoring energy consumption before and after time 30 in Figure 10, we find that the overall energy consumption of the social network remains largely stable, even after the fault recovery mechanism is engaged. This stability highlights the robustness and adaptability of our controller in handling agent dynamics, effectively maintaining network stability and efficient operation in practical applications.

It is important to note that in Figures 3–5, 7, and 9, each line represents the change in the cooperation level of each agent in the social network. In Figures 6, 8, and 10, each line represents the energy consumption required for the controller to influence each agent.

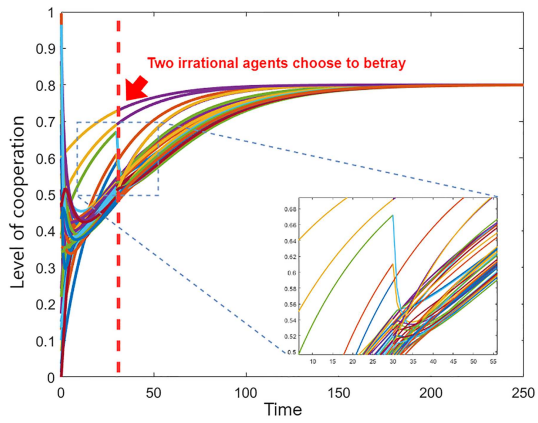


**Figure 9** (Color online) At time 30, two irrational agents betray and the failure is restored.

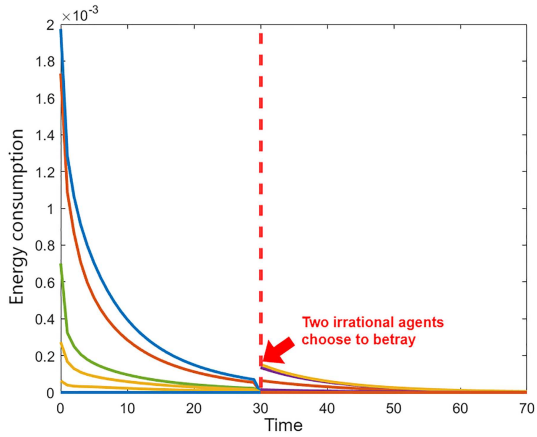


**Figure 10** (Color online) Square of the energy consumption required when two irrational agents are replaced at time 30.

## 6 Conclusion

In this paper, we explore the dynamics of cooperative behavior in social networks, emphasizing the use of the CAIPD model to facilitate widespread collaboration. The CAIPD model, newly introduced into existing research, has demonstrated its effectiveness in sustaining cooperation in complex networks. However, it is common for social networks to display a mix of competition and cooperation.

Our approach involves utilizing the CAIPD model to assess the evolution of cooperation among network agents, making all agents sensitive to external influences. This sensitivity enables us to induce cooperation in group games by applying optimal external influences on a small number of irrational agents. We compare this approach with traditional anti-step controllers to demonstrate the superiority of our optimal control method. However, during cooperative processes, affected irrational agents may occasionally shift from cooperation to betrayal. To address this, we have developed a heuristic adjustment algorithm that formulates an optimal inductive strategy, restoring cooperation robustness. This mechanism ensures that even if an irrational agent betrays, the entire social network can remain stable and continue to achieve the intended cooperation.

Studying collaborative control in social networks holds significant practical implications. For instance, politicians may seek to influence social relationships to propagate their viewpoints across the entire social network. Similarly, governments might offer tax incentives to exemplary businesses, encouraging competitors to automatically emulate these successful behaviors. Therefore, controlling social networks has broad applications in real-life scenarios and policy formulation.

**Acknowledgements** This work was supported in part by National Science Fund for Distinguished Young Scholars (Grant No. 62025602), National Natural Science Foundation of China (Grant Nos. U22B2036, 62373302), Fundamental Research Funds for the Central Universities (Grant Nos. G2024WD0151, D5000240309), Tencent Foundation, and XPLORER PRIZE.

**References**

1 Zhang X M, Han Q L, Ge X, et al. Networked control systems: a survey of trends and techniques. IEEE CAA J Autom Sin, 2019, 7: 1–17
2 Wei X, Zhang Y, Fan Y, et al. Online social network information dissemination integrating overconfidence and evolutionary game theory. IEEE Access, 2021, 9: 90061–90074
3 Garcia-Zamora D, Labella A, Ding W, et al. Large-scale group decision making: a systematic review and a critical analysis. IEEE CAA J Autom Sin, 2022, 9: 949–966
4 Axelrod R, Hamilton W D. The evolution of cooperation. Science, 1981, 211: 1390–1396
5 Zimmermann M G, Eguíluz V M. Cooperation, social networks, and the emergence of leadership in a prisoners dilemma with adaptive local interactions. Phys Rev E, 2005, 72: 056118
6 Santos F C, Santos M D, Pacheco J M. Social diversity promotes the emergence of cooperation in public goods games. Nature, 2008, 454: 213–216
7 Wang J, Xia C. Reputation evaluation and its impact on the human cooperation a recent survey. Europhys Lett, 2023, 141: 21001
8 Xia C, Wang J, Perc M, et al. Reputation and reciprocity. Phys Life Rev, 2023, 46: 8–45
9 Foderaro G, Ferrari S, Wettergren T A. Distributed optimal control for multi-agent trajectory optimization. Automatica, 2014, 50: 149–154
10 Bloembergen D, Sahraei B R, Bou-Ammar H, et al. Influencing social networks: an optimal control study. In: Proceedings of European Conference on Artificial Intelligence (ECAI), 2014. 14: 105–110
11 Zhu Y, Xia C, Wang Z, et al. Networked decision-making dynamics based on fair, extortionate and generous strategies in iterated public goods games. IEEE Trans Netw Sci Eng, 2022, 9: 2450–2462

12 Zhu Y, Xia C, Chen Z. Nash equilibrium in iterated multiplayer games under asynchronous best-response dynamics. IEEE Trans Automat Contr, 2023, 68: 5798–5805
13 Wang J, Hong Y, Wang J, et al. Cooperative and competitive multi-agent systems: from optimization to games. IEEE CAA J Autom Sin, 2022, 9: 763–783
14 Mazouchi M, Naghibi-Sistani M B, Sani S K H. A novel distributed optimal adaptive control algorithm for nonlinear multi-agent differential graphical games. IEEE CAA J Autom Sin, 2017, 5: 331–341
15 Odeh S, Caianiello P. Population dynamics in the iterated prisoner dilemma with prior commitment. In: Proceedings of the 6th International Conference on Social Networks Analysis, Management and Security (SNAMS), 2019. 256–261
16 Zhu Y, Zhang Z, Xia C, et al. Equilibrium analysis and incentive-based control of the anticoordinating networked game dynamics. Automatica, 2023, 147: 110707
17 Buzna L, Peters K, Ammoser H, et al. Efficient response to cascading disaster spreading. Phys Rev E, 2007, 75: 056107
18 Shang Y. Localized recovery of complex networks against failure. Sci Rep, 2016, 6: 30521
19 Saunders A, Ashlock D, Greensmith J. Necrotic behavioral control of agent behavior in the iterated prisoners dilemma. In: Proceedings of IEEE Congress on Evolutionary Computation (CEC), 2021. 1593–1600
20 Tuyls K, Hoen P J , Vanschoenwinkel B. An evolutionary dynamical analysis of multi-agent learning in iterated games. Auton Agent Multi-Agent Syst, 2006, 12: 115–153
21 Carneiro Y C, dos Santos J P C, Belgamo A, et al. A hybrid application for prisoner's dilemma game. In: Proceedings of XVII Latin American Conference on Learning Technologies (LACLO), 2022. 1–8
22 Ranjbar-Sahraei B, Ammar H B, Bloembergen D, et al. Evolution of cooperation in arbitrary complex networks. In: Proceedings of the International Conference on Autonomous Agents and Multi-agent Systems. 2014. 677–684
23 Jadbabaie A, Lin J, Morse A S. Coordination of groups of mobile autonomous agents using nearest neighbor rules. IEEE Trans Automat Contr, 2003, 48: 988–1001
24 Park S, Deyst J, How J P. Performance and Lyapunov stability of a nonlinear path following guidance method. J Guid Control Dyn, 2007, 30: 1718–1728
25 Barabási A L, Albert R. Emergence of scaling in random networks. Science, 1999, 286: 509–512